It is well established that the oxygen isotope shift coefficient α_O in doped high-T_c superconductors (HTSC) increases substantially with decreasing T_c, when the carrier doping is reduced from optimal levels[7,12,14]. In some cases α_O exceeds the conventional value of 0.5 at low carrier doping, and even slightly negative values have been reported close to optimal doping[9,10,12]. This suggests a non-vanishing coupling between the electrons and certain high-frequency oxygen phonon modes (see, for example, refs 15, 21–23). Nevertheless, the small oxygen isotope shift, together with the high T_c for optimally doped HTSC cannot be explained using the conventional theory of Bardeen, Cooper and Schrieffer (BCS theory), and therefore a more complex phononic and/or non-phononic (polaronic/magnetic) coupling mechanism has to be considered[15]. As early as 1979 a group in Dubna[24] had already predicted that anharmonic lattice vibrations may enhance the electron–phonon coupling, causing a substantial increase of T_c. In 1987 Plakida et al.[21] proposed an anharmonic model in which the Cu O planar tilting modes, a characteristic feature of perovskites, are considered to be important for electron–phonon pairing in HTSC. Moreover, it was suggested by one of us[15] that the apex oxygen motion is anharmonic and that the holes in the CuO_2 layers next to the apical oxygens are largely responsible for superconductivity in these materials. Indeed, several experiments (see, for example, refs 15, 21, 22), as well as computer simulations[23] suggest, that particular anharmonic oxygen modes are involved in the electron pairing. For instance, recent Raman investigations[25] on $YBa_2Cu_3O_{6+x}$ revealed that the apex oxygen mode is anharmonic. Furthermore, anharmonicity[21,22] may account for a large T_c and a small isotope effect coefficient α, and also provides an explanation for the extremely large as well as for the small negative oxygen isotope shifts observed in doped cuprates. It is therefore not surprising that in optimally doped $YBa_2Cu_3O_{6+x}$ the contribution of the apical (chain) oxygen sites to the total oxygen isotope shift is rather small (<20%), in view of the fact that the apex motion is anharmonic[15,25].

Our results clearly demonstrate that the oxygen sites in the CuO_2 planes mainly contribute to the total but small oxygen isotope effect in $YBa_2Cu_3O_{6+x}$ samples close to optimal doping. This suggests that theories of electron pairing in high-temperature superconductors have to consider a phononic contribution, in which the planar tilting or buckling modes in the CuO_2 layers play an essential role[21,22]. □

1. Batlogg, B. et al. Phys. Rev. Lett. 58, 2333–2336 (1987).
2. Bourne, L. C. et al. Phys. Rev. Lett. 58, 2337–2339 (1987).
3. Bourne, L. C., Zettl, A., Barbee, T. W. & Cohen, M. L. Phys. Rev. B36, 3990–3993 (1987).
4. Leary, K. J. et al. Phys. Rev. Lett. 59, 1236–1239 (1987).
5. Morris, D. E., Kuroda, R. M., Markelz, A. G., Nickel, J. H. & Wei, J. Y. T. Phys. Rev. B37, 5936–5939 (1988).
6. Hoen, S. et al. Phys. Rev. B39, 2269–2278 (1989).
7. Crawford, M. K., Kunchur, M. N., Farneth, W. E., McCaron E. M. & Poon, S. J. Phys. Rev. B41, 282–287 (1990).
8. Franck, J. P., Jung, J., Mohamed, M. A-K., Gygax, S. & Sproule, G. I. Phys. Rev. B44, 5318 5321 (1991).
9. Bornemann, H. J. & Morris, D. E. Phys. Rev. B44, 5322–5325 (1991).
10. Bornemann, H. J., Morris, D. E. & Liu, H. B. Physica C182, 132–136 (1991).
11. Babushkina, N. et al. Physica C185–189, 901–902 (1991).
12. Bornemann, H, J., Morris, D. E., Liu, H. B. & Narwankar, P. K. Physica C191, 211–218 (1992).
13. Nickel, J. H., Morris, D. E. & Ager, J. W. Phys. Rev. Lett. 70, 81–84 (1993).
14. Franck, J. P., Harker, S. & Brewer, J. H. Phys. Rev. Lett. 71, 283–286 (1993).
15. Müller, K. A. Z. Phys. B80, 193–201 (1990).
16. Conder, K., Kaldis, E., Maciejewski, M., Müller, K. A. & Steigmeier, E. F. Physica C210, 282–288 (1993).
17. Morris, D. E. et al. Phys. Rev. B44, 9556–9560 (1991).
18. Conder, K. Rusiecki, S. & Kaldis, E. Mater. Res. Bull. 24, 581–587 (1989).
19. Conder, K., Krüger, Ch., Kaldis, E., Zech, D. & Keller, H. Physica C225, 13–20 (1994).
20. Zech, D., Keller, H., Müller, K. A., Conder, K. & Kaldis, E. in Proc. Int. Conf. High-Temperature Superconductivity M²HTSC IV Grenoble, France 1994; Physica C (in the press).
21. Plakida, N. A., Aksenov, V. L. & Drechsler, S. L. Europhys. Lett. 4, 1309–1314 (1987).
22. Crespi, V. H. & Cohen, M. L. Phys. Rev. B48, 398–406 (1993).
23. Frick, M., Morgenstern, I. & von der Linden, W. Z. Phys. B82, 339–345 (1991).
24. Vujičić, G. M., Aksenov, V. L., Plakida, N. M. & Stamenković, S. Phys. Lett. 73A, 439–441 (1979).
25. Ruani, G. et al. Physica C226, 101–105 (1994).

Classification of chemical bonds based on topological analysis of electron localization functions

B. Silvi & A. Savin

Laboratoire de Dynamique des Interactions Moléculaires, UPR271, Université Pierre et Marie Curie, 4 Place Jussieu, 75252 Paris cédex, France

THE definitions currently used to classify chemical bonds (in terms of bond order, covalency versus ionicity and so forth) are derived from approximate theories[1–3] and are often imprecise. Here we outline a first step towards a more rigorous means of classification based on topological analysis of local quantum-mechanical functions related to the Pauli exclusion principle. The local maxima of these functions define 'localization attractors', of which there are only three basic types: bonding, non-bonding and core. Bonding attractors lie between the core attractors (which themselves surround the atomic nuclei) and characterize the shared-electron interactions. The number of bond attractors is related to the bond multiplicity. The spatial organization of localization attractors provides a basis for a well-defined classification of bonds, allowing an absolute characterization of covalency versus ionicity to be obtained from observable properties such as electron densities.

The valence theory of Lewis[1] remains the basis for most modern ideas on and classifications of the chemical bond[2,3]. Most such classifications rely on molecular-orbital and valence-bond theories within schemes involving the linear combination of atomic orbitals (LCAO)[4,5].

The characterization of chemical bonds is a qualitative rather than a quantitative exercise, and the question is how one can distil the relevant information from experiment or from quantum-chemical calculations. The differential topology analysis of local scalar functions is a well-established mathematical approach that is well suited to handling this problem[6]. For a continuous, differentiable function $g(r)$ defined for any point in three-dimensional (R^3) space, the gradient $\mathbf{X}$ defines a vector field. The theory of gradient vector fields has been successfully developed as a part of dynamical systems theory[6,7] (see, for instance, Abraham and Marsden[8] for a good introduction to the subject). Using this approach, one can identify trajectories of which the points corresponding to $t \to -\infty$ and $t \to \infty$ are respectively the α- and ω- limits. The set of ω-limits is the set of the attractors of the dynamical system. The basin of an attractor is the set of points for which this attractor is the ω-limit. This approach has been pioneered for chemical bonding by Bader[9] who emphasized the role of the electron density $\rho(r)$. Definition of attractors allows one to define basins which are recognized as atoms in molecules. Further analysis allows one to identify objects associated with bonds. Alternatively, the topological type of density domains bounded by isosurfaces can be considered. When the threshold defining the bounding isosurface is varied, the shape of a given density domain may or may not change. A change of topological type that occurs at a critical value of the threshold is called a bifurcation. The characterization of these

shapes and applications to chemical systems has been reviewed by Mezey[10].

Electron density alone does not easily reveal the consequences of the Pauli exclusion principle on the bonding. The valence-shell electron-pair repulsion (VSEPR) theory[11] indicates that the Pauli principle is important for understanding chemical bonding. This theory has been reformulated in terms of maxima of $-\nabla^2\rho(r)$ (ref. 12). The seminal works of Artmann[13], Lennard-Jones[14], and Bader and Stephens[15] have produced a series of localization functions which attempt to measure the Pauli repulsion by considering the Fermi hole (compare Luken and Culberson[16] and Becke and Edgecombe[17]). An alternative interpretation of these so-called electron localization functions, $\eta(r)$, can be made by considering the excess local kinetic energy due to Pauli repulsion[18]. The local kinetic energy $K(r)$ is:

$$K(r) = -\frac{1}{2}\sum_{i=1}^{N}\int \Psi^*\nabla_i^2\Psi \, d\tau'$$

where Ψ is an N-particle wavefunction and the prime indicates that the integration is performed over the space and spin coordinates of all particles but one.

Consider a system of fermions and a system of bosons with identical densities. The ground-state local kinetic energy of the non-interacting bosonic system is a lower bound to the local kinetic energy of the fermionic one[19]. The excess local kinetic energy due to the Pauli principle is just the difference between the two. Where electrons are alone or form pairs of opposite spins, the Pauli principle has little influence on their behaviour and they almost behave like bosons. In such regions the excess local kinetic energy has a low value. For practical purposes, we will require localization functions to have their maxima corresponding to this "bosonic" regime. The actual values of localization functions are calculated from approximate wavefunctions provided by quantum chemistry. However, it should be possible to derive procedures that will allow their determination from experimental densities[20,21] or from the measurement of the Wigner function[22].

For gradient-type dynamical systems, zero-dimensional attractors are generic[7]. In differential topology, generic means typical; a generic property holds for most systems, but it can be violated in exceptional cases. Nevertheless, for examples that are relevant to chemistry, the system could belong to a continuous symmetry group which in turn implies that the attractor could
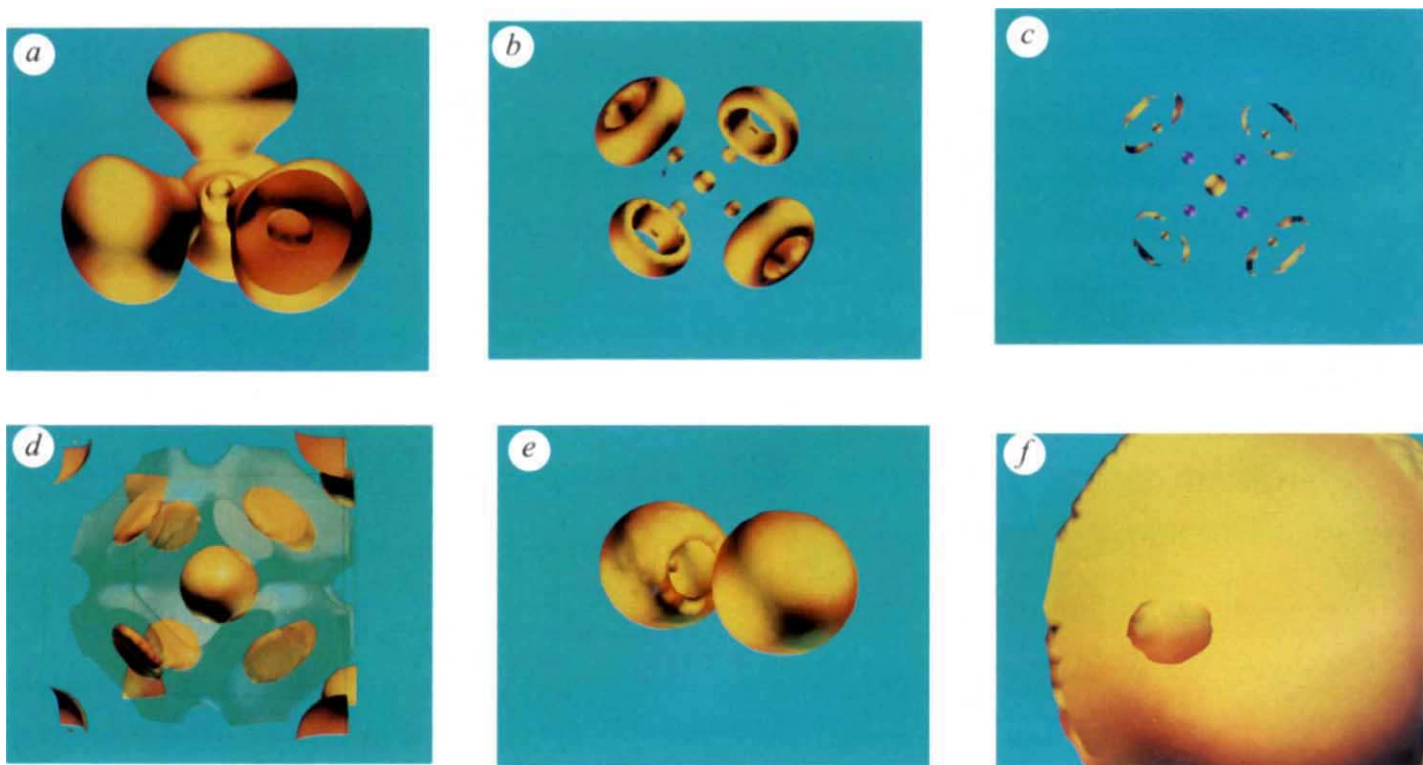

FIG. 1 Localization domains of CF_4 (a–c), Li (d), LiF (e) and LiH (f). a–c, Reduction of the localization domains of CF_4. Below ELF = 0.37 (where ELF is the localization function; see text) there are six localization domains: five core and one valence. The bifurcation at ELF = 0.37 splits the common valence domain into four atomic ones. The ELF = 0.75 map (a) shows the carbon core surrounded by the four fluorine valence domains; the front cutting plane has been chosen so that a fluorine core domain can be seen. The bonding attractors are responsible for the bulges towards the carbon centre. A further bifurcation occurs at ELF = 0.78, giving rise to bonding point attractors and non-bonding ring attractor domains as shown in b (ELF = 0.85). Each ring is itself resolved into three non-bonding point attractors for ELF > 0.883. The bonding attractors at which ELF = 0.879 are represented by purple spheres because the bounding isosurface 0.885 only encapsulates the core and non-bonding attractors. b.c.c. lithium: the core and bonding attractors are located at the 8a (centre and vertices of the cubic lattice) and 8c

(midpoints between the centre and the vertices) positions respectively. Their domains are bounded by the ELF = 0.625 isosurfaces, and the ELF = 0.575 isosurface forms a network of channels connecting the bonding attractors. These bonding attractors are unsaturated because there are eight per cell sharing two valence electrons. For LiF e, the localization domains shown are bounded by the ELF = 0.84 isosurface. The fluorine valence domain (which is almost spherical at lower ELF values) shows a hole in front of the lithium core; increasing the threshold leads to a single attractor lying on the internuclear axis on the side of the fluorine core that is away from the lithium. The ELF = 0.999 iso-surfaces of LiH (f) encapsulate, on the one hand, the lithium core and, on the other hand, a very large area which extends, in principle, to infinity. The calculation of the grid points has been limited to a box of dimensions $7 \times 7 \times$ a.u., therefore only one face of the largest domain can be seen. The roughness of the surface is due to interpolation limitations and a density cutoff.

be no longer zero-dimensional. We now consider some ideal localization functions in the most general case. The integral of the charge density over the basin of an attractor provides the number of electrons that belong to that basin. The Pauli principle implies that at most two electrons with opposite spins should be found in a basin in the absence of symmetry. An attractor for which $q(A)$ is less than 2 will be called hereafter an unsaturated attractor. A "loge", in the sense of Daudel[23], is the basin of a saturated attractor.

The space symmetry of atoms ($SO(3)$ group) and of linear molecules ($C_{\infty v}$ group), together with the Pauli principle, imply the following atomic attractors are either single point attractors located at the nucleus (K-shell attractor) or concentric spherical attractors due to the degeneracy of the off-centred attractors. The outer spherical attractor is the valence shell. In linear molecules, one can find point attractors on the internuclear axis and ring attractors centred on the axis. Spherical and ring attractors can be resolved into at least one point attractor when the symmetry is broken. Point, ring and spherical attractors are the generic topological types allowed by symmetry. They will, therefore, form the basis of our topological theory of the chemical bond.

The formation of a molecule or crystal from atoms breaks the $SO(3)$ symmetry, and therefore leads to competition between attractors which are reorganized accordingly. To describe the chemical bond, we will first consider the f-localization domain

which we define as the set of points for which the localization function is larger or equal to f. An f-localization domain contains at least one attractor. A localization domain encapsulating more than one attractor will be called reducible, whereas an irreducible localization domain contains one (and only one) attractor. A localization domain is bounded by the isosurface $\eta(r) = f$. When f is varied, the localization domains undergo deformations which do not alter their topological type, if they are irreducible, whereas for reducible localization domains bifurcations occur for critical values of f. A bifurcation yields a reduction of the localization domain into several localization domains containing fewer attractors. The spatial arrangement of the irreducible localization domains is the corner-stone of our classification of chemical bonds. From a chemical point of view there are three types of attractors: core, bonding (located between the core attractors of different atoms) and non-bonding. Following Bader[9], there are basically two kinds of bonding interaction: shared-electron interaction and closed-shell (or more generally, unshared-electron) interaction. Covalent, dative and metallic bonds are subclasses of the shared-electron interaction whereas ionic, hydrogen, electrostatic and van der Waals bonds belong to the other class. For shared-electron interaction there is always at least one bond attractor between the core attractors of the atoms involved in the bond. The case of hydrogen is special because it has no core attractor, and so the above classification
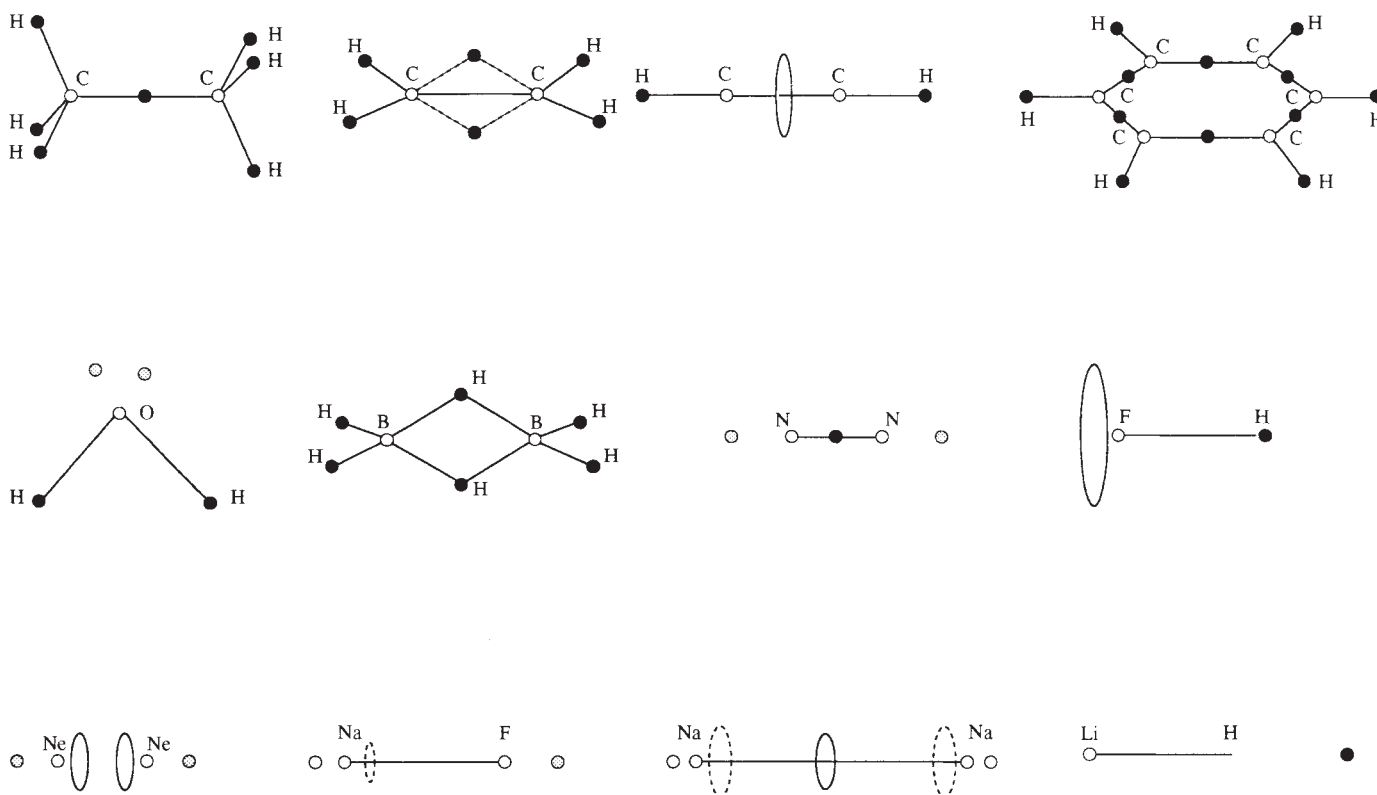

FIG. 2 Bonding diagrams of: (top row) C_2H_6, C_2H_4, C_2H_2 and C_6H_6; (middle row) H_2O, B_2H_6, N_2 and HF; (bottom row) Ne_2, NaF, Na_2 and LiH. The core, bonding and non-bonding point attractors are presented by white, black and grey dots, respectively. Core ring attractors are drawn in dashed lines, valence attractors in solid lines. The conventional structure is given by solid lines joining the nuclei. In shared-electron interactions involving hydrogen (for example, C_2H_6), the bond attractors are very near the protons whereas for hydrides such as LiH, the localization of the attractor is not very reliable because the localization function is very close to 1, in a domain that extends to infinity. C_2H_4 and B_2H_6 have very similar attractor patterns, which gives support to the

'banana' representation of the double bond in ethylene. The number of electrons related to a point attractor lying on a symmetry element may be more than two: at most, twice the order of the element. Conversely, an electron pair may give rise to a ring attractor. The triple bond attractors are degenerated onto a ring in acetylene, but correspond to a single point in N_2; the bonding ring attractor of Na_2 is related to a single pair. The diagrams for Na_2 and NaF show how symmetry-breaking with respect to the free ion splits the Na L-shell sphere attractor into a point and a ring. The diagram of Ne_2 corresponds to a repulsive interaction, the internuclear separation having been constrained to 1 Å.

criteria cannot be applied. However, the shape of the localization domains around the proton provides information which could be useful in this respect. When hydrogen gets a more negative character, its localization domain becomes larger (for a given value of the threshold defining the bounding isosurface).

The results used to illustrate our theory have been selected from about 100 typical systems for which the Hartree–Fock wavefunction and the ELF (ref. 17) localization function have been calculated with the *ab initio* program CRYSTAL92 (ref. 24) and visualized with the data analyser software SciAn (ref. 25). For a single determinental wavefunction built from Hartree–Fock or Kohn–Sham orbitals φ_i,

$$ELF = \frac{1}{1 + \left(\dfrac{D}{D_h}\right)^2}$$

with

$$D = \frac{1}{2}\sum_i |\nabla\varphi_i|^2 - \frac{1}{8}\frac{|\nabla\rho|^2}{\rho}$$

$$D_h = \frac{3}{10}(3\pi^2)^{5/3}\rho^{5/3}$$

is calculated on a grid in the three-dimensional space. ELF has values between 0 and 1, where 1 corresponds to perfect localization. Figure 1 illustrates the idea of localization domains and shows how efficient graphic facilities can help to perform the analysis. The reduction of the localization domains of CF_4 is consistent with the covalent bonding suggested by standard methods. The metallic bond is illustrated by the lithium body-centred cubic (b.c.c.) structure. Trajectories connecting the bond attractors form a three-dimensional network and pass through the saddle points. Along these paths, the value of the localization function remains nearly constant. This feature is observed for all the metallic phases we have investigated and seems to be characteristic of the metallic bond.

The attractors of 12 typical systems have been localized by a gradient search technique. The organization of these attractors is shown in Fig. 2. In both systems belonging to the shared-electron interaction set, there is always a point or ring valence attractor on the bond path whereas for the unshared-electron interaction there is nothing between the core attractors. Non-bonding lone-pair attractors are either point attractors as in H_2O, N_2 and NaF, or ring attractors in the case of HF, or both for Ne_2.

The approach presented here is an additional step towards a non-empirical basis for the classification of chemical bonds. It complements and augments the theory of Bader[9]. The integration of the electron density over the localization basins is in progress and should provide further information on the bond multiplicity and on the attractor saturation. □

1. Lewis, G. N. *Valence and the Structure of Atoms and Molecules* (Dover, New York, 1966).
2. Kossel, A. *Ann. Physik Chemie* **49**, 229–362 (1916).
3. Langmuir, I. *J. Am. chem. Soc.* **41**, 868–934 (1919).
4. Pauling, L. *The Nature of the Chemical Bond* (Cornell Univ. Press, 1960).
5. Coulson, C. A. *Valence* (Clarendon Press, Oxford, 1952).
6. Thom, R. *Stabilité Structurelle et Morphogénèse* (Intereditions, Paris, 1972).
7. Palis, J. & Smale, S. *Proc. 14th Symp. Pure Mathematics Global Analysis* (eds Chern, S. S. & Smale, S.) 223–231 (American Mathematical Soc., Providence, 1970).
8. Abraham, R. & Marsden, J. E. *Foundation of Mechanics* 507–571 (Addison-Wesley, Redwood, 1987).
9. Bader, R. F. W. *Atoms in Molecules: A Quantum Theory* (Oxford Univ. Press, 1990).
10. Mezey, P. in *Reviews in Computational Chemistry* (eds Lipkowitz, K. B. & Boyd, D. B.) Vol. 1 (VCH, New York, 1990).
11. Gillespie, R. J. *Molecular Geometry* (van Nostrand, London, 1972).
12. Bader, R. F. W., Gillespie, R. J. & McDougall, P. J. *J. Am. chem. Soc.* **110**, 7329–7336 (1988).
13. Artmann, K. *Z. Naturf.* **1**, 426–432 (1946).
14. Lennard-Jones, J. *Proc. R. Soc.* A**198**, 1–13, 14–26 (1949).
15. Bader, R. F. W. & Stephens, M. E. *J. Am. chem. Soc.* **97**, 7391–7399 (1975).
16. Luken, W. L. & Culberson, J. C. *Int. J. quant. Chem.* **16**, 265–276 (1982).
17. Becke, A. D. & Edgecombe, K. E. *J. chem. Phys.* **92**, 5397–5403 (1990).
18. Savin, A., Jepsen, J., Andersen, O. K., Preuss, H. & von Schnering, H. G. *Angew. Chem.* **31**, 187–188 (1992).
19. Tal, Y. & Bader, R. F. W. *Int. J. quant. Chem.* **S12**, 153–168 (1978).
20. Levy, M. *Proc. natn. Acad. Sci. U.S.A.* **76**, 6062–6065 (1979).
21. Massa, L., Goldberg, M., Frishberg, C., Boehme R. F. & La Placa, S. J. *Phys. Rev. Lett.* **55**, 622–625 (1985).
22. Royer, A. *Phys. Rev. Lett.* **55**, 2745–2748 (1985).
23. Daudel, R. *Quantum Theory of the Chemical Bond* (Reidel, Dordrecht, 1974).
24. Dovesi, R., Saunders, V. R. & Roetti, C. *CRYSTAL 92* (Theoretical Chemistry Group, Univ. Turin & SERC Daresbury Laboratory, 1992).
25. Pepke, E., Murray, J., Lyons, J. & Hwu, T.-Z. *SciAn* (Supercomputer Computations Res. Inst., Florida State Univ., Tallahassee, Florida, 1993).

Response of benthic oxygen demand to particulate organic carbon supply in the deep sea near Bermuda

F. L. Sayles, W. R. Martin & W. G. Deuser

Department of Marine Chemistry and Geochemistry, Woods Hole Oceanographic Institution, Woods Hole, Massachusetts 02543, USA

OVER the past decade an increasing body of evidence has accumulated indicating that much, perhaps most, of the deep sea floor is an environment of substantial temporal variability[1–4]. This variability is driven largely by seasonal changes of processes occurring in the surface waters[2,3,5]. The coupling of the deep sea floor environment to the surface waters is the result of rapid vertical transport of particulate matter through the water column[6–8], affording only limited time for degradation before arrival at the sea floor. Studies in the Pacific Ocean have indicated that temporal variations in particulate organic carbon fluxes to the sea floor are accompanied by temporal variability in sediment oxygen demand by as much as a factor of four[1,2]. We report here time-series studies of oxygen fluxes into the sediments of the oligotrophic Atlantic near Bermuda which contrast sharply with these previous reports. At the Bermuda site, despite large seasonal variations in particulate organic carbon fluxes, *in situ* measured sediment oxygen consumption does not vary significantly. These results imply that large areas of the sea floor may be characterized by seasonally invariant sediment oxygen demand.

Temporal variations in the fluxes of, and response to, particulate matter reaching the sea floor have been observed in a variety of studies. Annual variations in fluxes of up to a factor of ten have been documented in continental margin[2,6,9,10] and open ocean environments[1,3,7,11]. In virtually all cases, particle flux variability has been linked to annual cycles of productivity in the overlying surface waters. The physical and chemical characteristics of material accumulating on the sea floor also exhibit short-term temporal variability. The sudden appearance of aggregates of phytodetritus on the surface of deep-sea sediment has been documented photographically at sites in both the northeast Atlantic[8,12] and eastern Pacific[13]. These events occur on an annual cycle and have been attributed to the rapid delivery of sinking particulate matter from surface blooms[8,12]. The presence of pigments and other rapidly degraded organic compounds in aggregates indicates that the material has undergone relatively little degradation before reaching the sea floor[4,14]. Studies of the arrival and disappearance of material from a particulate pulse on the Vöring Plateau (Norwegian Sea) suggest that the response of the benthic community can occur within days[15]. There is also strong evidence of changes in benthic metabolic activity associ-